Journal of Macromolecular Science, Part A
Publication details, including instructions for authors and subscription information:
http://www.informaworld.com/smpp/title~content=t713597274

Composites of Polystyrene Sulfonic Acid (PSSA)-Polyaniline and Montmorillonite Clay: Synthesis and Characterization

Yu-Feng Li[ab]; Yun-Pu Wang[a]; Xiao-Hui Gao[b]; Jing-Min Gao[a]
[a] Gansu Key Laboratory of Polymer Materials, Institute of Polymer, Northwest Normal University, Lanzhou, P. R. China [b] Chemistry and Chemical Engineering College, Qiqihar University, Qiqihar, P. R. China

To cite this Article Li, Yu-Feng , Wang, Yun-Pu , Gao, Xiao-Hui and Gao, Jing-Min(2006) 'Composites of Polystyrene Sulfonic Acid (PSSA)-Polyaniline and Montmorillonite Clay: Synthesis and Characterization', Journal of Macromolecular Science, Part A, 43: 2, 405 — 415
To link to this Article: DOI: 10.1080/10601320500437326
URL: http://dx.doi.org/10.1080/10601320500437326

Journal of Macromolecular Science®, Part A: Pure and Applied Chemistry, 43:405–415, 2006

ISSN 1060-1325 print/1520-5738 online
DOI: 10.1080/10601320500437326

Composites of Polystyrene Sulfonic Acid (PSSA)-Polyaniline and Montmorillonite Clay: Synthesis and Characterization

YU-FENG LI,[1,2] YUN-PU WANG,[1] XIAO-HUI GAO,[2] AND JING-MIN GAO[1]

[1]Gansu Key Laboratory of Polymer Materials, Institute of Polymer, Northwest Normal University, Lanzhou, P. R. China
[2]Chemistry and Chemical Engineering College, Qiqihar University, Qiqihar, P. R. China

Polystyrene sulfonic acid (PSSA) doped water-soluble polyaniline (PANI)/montmorillonite (MMT) clay composites were synthesized by intercalation polymerization in aqueous medium. The properties of the composites were characterized by X-ray diffraction (XRD), transmission electron microscope (TEM), Fourier-transform infrared spectroscopy (FT-IR), thermogravimetric analysis (TGA), differential scanning calorimetry (DSC), X-ray photoelectron spectroscopy (XPS) and conductivity measurement. The results show that the composite has a mixed nanomorphology and exfoliated silicate nanolayers of MMT clay dispersed in the polyaniline matrix. This composite is more thermal stable than that without clay samples and results in good stable temperature-dependent dc conductivity [$\sigma_{dc}(T)$] as temperature changed.

Keywords polystyrene sulfonic acid, polyaniline, montmorillonite, composite

Introduction

The composites of conducting polymers and inorganic materials have attracted the interest of researchers recently (1, 2), because the composites' properties will be improved and some new synergistic properties were found that couldn't be attained from individual materials (3). Polyaniline (PANI) has many advantages: relatively cheap, easy to synthesize, environmental stability and controlled conductivity, so the PANI is regarded as the most promising conducting polymer material for commercial application (4). A large amount of PANI-inorganic composites have been synthesized and studied to enhance the overall properties and broadening the practical applications in the past few years, for example, PANI/V_2O_5 (5), PANI/TiO_2 (6–8), PANI/CdS (9), PANI/$VOPO_4 \cdot 2H_2O$ (10), PANI/graphite oxide (11), PANI/bentonite-vanadium oxide (12), PANI/Clay (13–19), etc.

Received March 2005; Accepted June 2005.
Address correspondence to Yun-Pu Wang, Gansu Key Laboratory of Polymer Materials, Institute of Polymer, Northwest Normal University, Lanzhou 730070, P. R. China. E-mail: lyf1170@163.com

Among inorganic materials, montmorillonite (MMT) clay has received a great deal of attention because of its unique layered structure. The monomer (aniline) can be introduced into the galleries by ion exchange and form extended chain of PANI in the interlayers by intercalacation polymerization (20, 21). We could study the chain structure, polymerization mechanism and conductivity of PANI in this system. Goddard et al. (22) characterized PANI/MMT clay nanocomposite by solid-state deuteron quadrupole echo and magic angle spinning NMR experiments. The results imply that polarons play an important role in the conductivity mechanism.

The PANI/MMT clay composites have also been proven to have many special properties such as electrical conductivity, thermal and mechanical stability, etc. (23). Lee et al. (24) demonstrated the PANI/Na^+-MMT nanocomposite are more thermally stable than those for a simple mixture. Lim et al. (25) studied the application of PANI/clay intercalated nanocomposites in electro-rheological fluids. The PANI–clay nanocomposite particles, which can form a columnar structure under an electric field, strongly enhance the mechanical rigidity of the suspensions. Yeh et al. (26) studied polyaniline-clay nanocomposites in the form of coatings with low clay loading on cold-rolled steel based on a series of electrochemical measurements, and found the nanocomposites was much superior in corrosion protection over those of conventional polyaniline.

In this paper, we report the synthesis and characterization of the composites of polystyrene sulfonic acid (PSSA) doped PANI and MMT clay. The results of X-ray diffraction (XRD) experiments indicating the MMT clay in the composites has an exfoliated layered structure. The transmission electron microscope (TEM) photograph showed a mixed nanomorphology and we observed many exfoliated silicate nanolayers of MMT clay dispersed in the polyaniline matrix. Fourier-transform infrared spectroscopy (FT-IR) confirmed the interaction between the PSSA-PANI chain and the surface of the MMT clay layer in the composite. The enhanced thermal stability is demonstrated by thermogravimetric analysis (TGA), differential scanning calorimetry (DSC) and temperature-dependent dc conductivity[σ_{dc}(T)]. The X-ray photoelectron spectroscopy (XPS) experiments of this system were also recorded. The synthesized PSSA-PANI is soluble in water. This is the first synthesis of water-soluble PANI/MMT clay composites and they are advantageous in potential aqueous medium applications.

Experimental

Materials

The reagents used in this study were of AR grade. Aniline was distilled under vacuum before use. The montmorillonite clay was purchased from Xinjiang clay mineral, prior to use, it was boiled with 1 M HCl and saturated NaCl solution sequentially to make Na^+-MMT. Water used in this investigation was deionized water.

Preparation of PSSA

Ten grams of noncrosslinking polystyrene was added into 100 ml concentrated H_2SO_4 (contain 0.2 g Ag_2SO_4) in ten parts and vigorously stirred for 4 h at 100°C. The mixtures were then pour into cooled water through a glass wool filter and the water solution was put into the refrigerator for 48 h at ~3°C. The precipitation was then encapsulated into a dialysis bag and washed with a large amount of deionized water many times

until there was no SO_4^{2-} determined. Brown PSSA was obtained by evaporating in a water bath and drying at about 90°C.

Preparation of PSSA-PANI/MMT Clay Composites

The Na^+-MMT was prepared in deionized water medium and sonicated using a ultrasonic generator to produce a fine aqueous dispersion. The PSSA, which at various molar ratios to aniline, was dissolved in deionized water and mixed with aniline, this monomer solution was then mixed with the clay solution at 80°C under nitrogen purge. After being magnetically stirred for 3 h, the mixture cooled down while stirring to ~3°C in an ice bath. A solution of ammonium peroxydisulfate (APS), at stoichiometric ratio, was dropped into the reactor to initiate the polymerization. The reaction lasted for 5 h after the color turned dark green and was terminated by adding excess acetone. The precipitate was filtered, washed with acetone and dried under vacuum at 40°C overnight. The dark green product was finally pulverized into a fine powder. For comparison, the PSSA-PANI materials without clay were synthesized by the same method. The obtained PSSA-PANI is soluble in water.

Characterization

XRD analyses were performed on a Shimadzu X-ray diffractometer (Model XRD-6000) with Cu-Kα radiation ($\lambda = 1.54$ Å) operating at 40 kV and 30 mA, the scanning rate is 6°/min. The materials for the XRD experiments were in ground powder form. The TEM photographs were taken by using a JEOL electron microscope (Model JEM-1200EX). For TEM observation, the ground fine powder of PSSA-PANI/MMT clay composite was dispersed in an acetone medium and sonicated for 1 h and then transferred to the copper grid. FT-IR spectroscopy was carried out with a Nicolet AVATAR 360 instrument using KBr pellets. The TGA experiments were performed by using a Pyris Diamond TG/DTA system (Perkin-Elmer instruments) under a nitrogen atmosphere at a heating rate of 10°C/min from 25°C to 800°C. The DSC experiments were performed by using a DT-40 TA system (Shimadzu instruments) at 10°C/min from 14°C to 500°C. The XPS data were measured on a PHI multi-function spectrometer (Model PHI5720). All binding energies were referenced by C 1s neutral carbon peak at 284.8 eV to compensate for surface charging effect. The electrical conductivity was recorded on an automatic component analyzer (Model TH2818) by a two-electrode technique. The samples were prepared with pellet form from fine powder under the pressure of 7.5×10^7Pa and coated with silver paint to minimize the contact resistance. A WJD-1 temperature-controlling device was used for measuring σ_{dc}(T) from 20°C to 100°C.

Results and Discussion

X-ray Diffraction

The powder X-ray diffraction patterns of the PSSA-PANI, PSSA-PANI/MMT clay and the Na^+-MMT clay samples are shown in Figure 1. The simple mixture of PSSA-PANI and MMT clay at the same amount of MMT content as the synthetic composite is used for comparison. We estimated the interlayer distance from the angular position 2θ of the observed peaks by using Bragg's Formula $n\lambda = 2d\sin\theta$. For Na^+-MMT clay samples, the diffraction peak is at $2\theta = 6.6°$and the interlayer distances is 13.3 Å. The

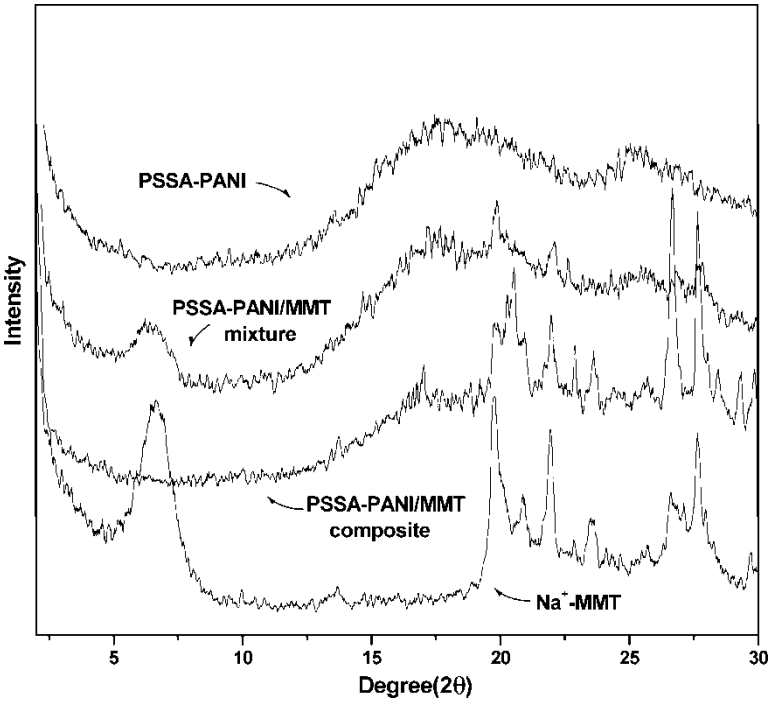

Figure 1. XRD patterns of the PSSA-PANI, PSSA-PANI/MMT and the Na^+-MMT clay samples.

PSSA-PANI/MMT mixture has a diffraction peak at the same angular position ($2\theta = 6.5^\circ$) as Na^+-MMT, and so has a similar interlayer distance (13.6Å). This result confirms the morphology of MMT couldn't be changed by a simple mix. For a PSSA-PANI/MMT clay composite, there is no diffraction peak in $2\theta = 2\text{–}10^\circ$ which

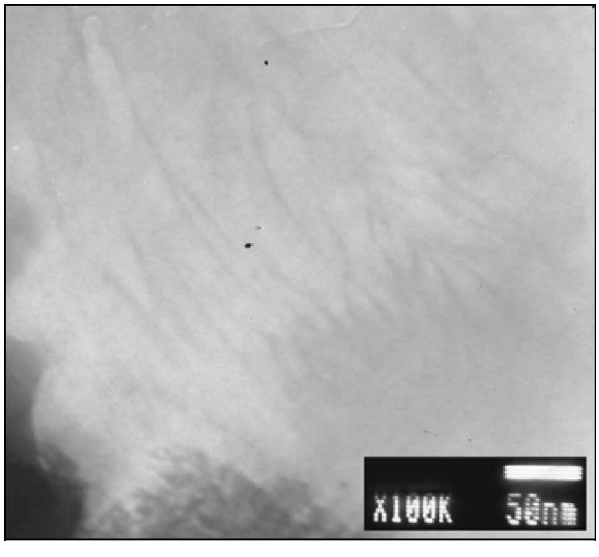

Figure 2. TEM photograph of PSSA-PANI/MMT composite (Magnification × 100 K).

indicates the possibility of having exfoliated silicate nanolayers of MMT clay dispersed in the polyaniline matrix due to the PSSA-PANI intercalating in the MMT clay layers.

TEM

The TEM photograph of PSSA-PANI/MMT composite is shown in Figure 2. It was observed that the composite has a mixed nanomorphology. Many silicate layers were found to be partially exfoliated in the polyaniline matrix, which confirms the result of XRD patterns. This is probably because the large molecular of PSSA-PANI propped the layers of montmorillonite clay open. There are also some multiplayer sections in the matrix, but they are so small and have few clay layers that do not have any observed d_{001} diffraction peaks in XRD patterns.

FT-IR Spectroscopy

Figure 3 compares the FT-IR results of the PSSA-PANI, PSSA-PANI/MMT clay mixture, PSSA-PANI/MMT clay composite and the Na^+-MMT clay samples. The peaks at 1305 (1308) cm^{-1} and 1219 (1238) cm^{-1} of the PSSA-PANI/MMT clay mixture(PSSA-PANI/MMT clay composite) are associated with the C–N stretching vibration. We

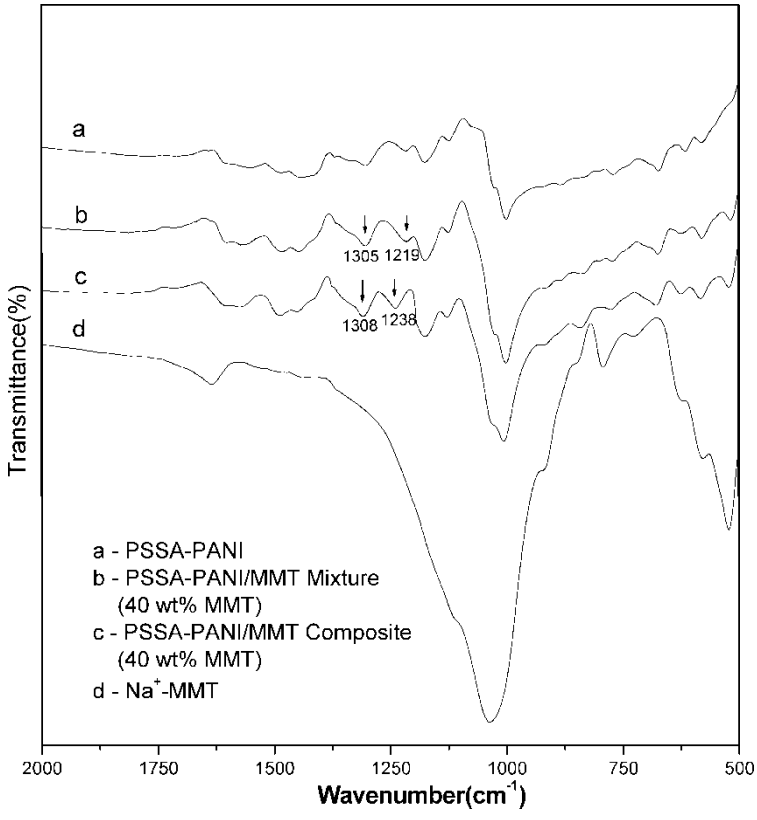

Figure 3. FT-IR spectroscopy of (a) PSSA-PANI, (b) PSSA-PANI/MMT clay mixture (40 wt% MMT), (c) PSSA-PANI/MMT clay composite (40 wt% MMT), and (d)Na^+-MMT.

observed that the frequency shift to higher wavenumbers ($1305 \rightarrow 1308\,cm^{-1}$, $1219 \rightarrow 1238\,cm^{-1}$) in the composite compared to the mixture and pure PSSA-PANI, which are in good agreement with the reports of Lee et al. (27) and Kim et al. (28). This is also believed to be caused by the interaction involving hydrogen bonding between the PSSA-PANI chain and the surface of the MMT clay layer. The frequency shift was not found in the mixture compared to pure PSSA-PANI and so demonstrated that the composition in molecular level between the PSSA-PANI chain and the surface of the MMT clay layer occurring in the composite only.

Thermal Stability Characteristics

The TGA thermograms of the PSSA-PANI, PSSA-PANI/MMT and the Na^+-MMT clay samples are shown in Figure 4. The PSSA molar concentration is in 1.25M. The major stages of the decomposition processes are summarized in Table 1. For PSSA-PANI, the first weight loss around 100°C (~6.6%) is the elimination of water and other volatiles.

The second stage in the temperature range 200–405°C is presumably due to the decomposition of excess dopant PSSA. The bound PSSA decomposes at about 414°C and then the PSSA-PANI itself decomposes (29). The TGA thermogram of the PSSA-PANI/MMT clay composite shows the similar weight loss, but the weight losses are lower in each major stage than that without clay samples, and the decomposition temperature of excess dopant PSSA (~237°C) and the bound PSSA (~441°C) increases by about 37°C and 27°C, respectively, relative to the bulk PANI. This result indicates the PSSA-PANI/MMT composite is more thermally stable than PSSA-PANI.

For comparison, the TG curves of PSSA-PANI/MMT clay composite at the different content of MMT and PSSA-PANI/MMT clay mixture at the same content of MMT are also shown in Figure 4. As the amount of MMT content is decreased, the decomposition

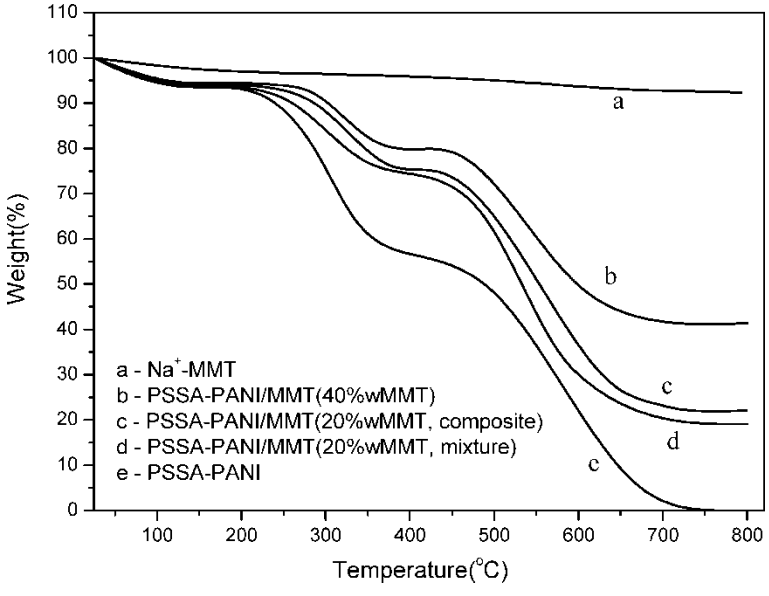

Figure 4. TGA thermograms of the PSSA-PANI, PSSA-PANI/MMT and the Na^+-MMT clay samples.

Table 1
The major stages of decomposition process for PSSA-PANI, PSSA-PANI/MMT composite and PSSA-PANI/MMT mixture containing the same amount of MMT (20 wt%)

Materials	Temperature range (°C)	Weight loss (%)
PSSA-PANI/MMT composite	25–117	5.7
(40 wt% MMT)	237–383	14.6
	441–711	38.7
PSSA-PANI/MMT composite	227–392	19.0
(20 wt% MMT)	426–725	53.2
PSSA-PANI/MMT mixture	211–405	19.7
(20 wt% MMT)	419–730	54.1
PSSA-PANI	25–143	6.6
	200–405	37.6
	414–733	55.8

temperatures are decreased and the weight losses are increased in every major stage. This result demonstrates that it is the MMT clay that protects the PSSA-PANI chains from degradation. The simple mixture of PSSA-PANI and MMT clay showed no enhancement in the thermal stability. The decomposition temperatures of the mixture are lower and has a completely decline like the pure PSSA-PANI. These results demonstrate that the enhanced thermal stability of PSSA-PANI/MMT clay composite is due to the attractive

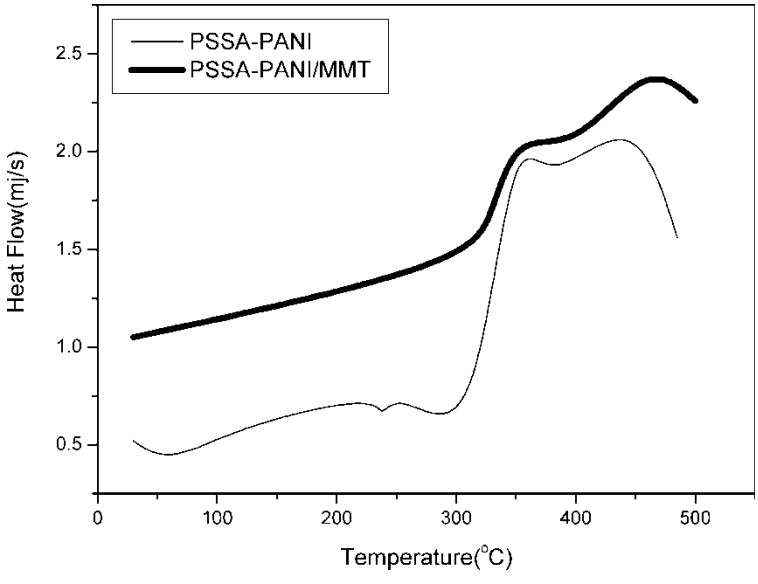

Figure 5. DSC curves of the PSSA-PANI and PSSA-PANI/MMT clay composite.

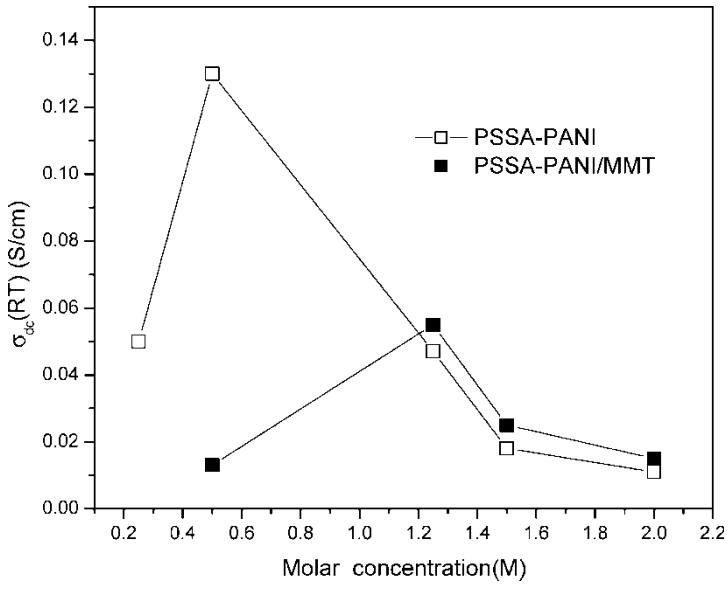

Figure 6. The room temperature σ_{dc} of the PSSA-PANI and PSSA-PANI/MMT clay composite.

interaction between the positive nitrogen of the PSSA-PANI and the partially negatively charged surface of the MMT clay by composition (24, 28).

The thermal stability is also confirmed by the results of DSC experiments in Figure 5. The curve of PSSA-PANI/MMT clay composite is more stable than the curve of PSSA-PANI, and the decomposition exotherm peaks of PSSA-PANI/MMT are weak and obviously shift to a higher temperature than that of the PSSA-PANI.

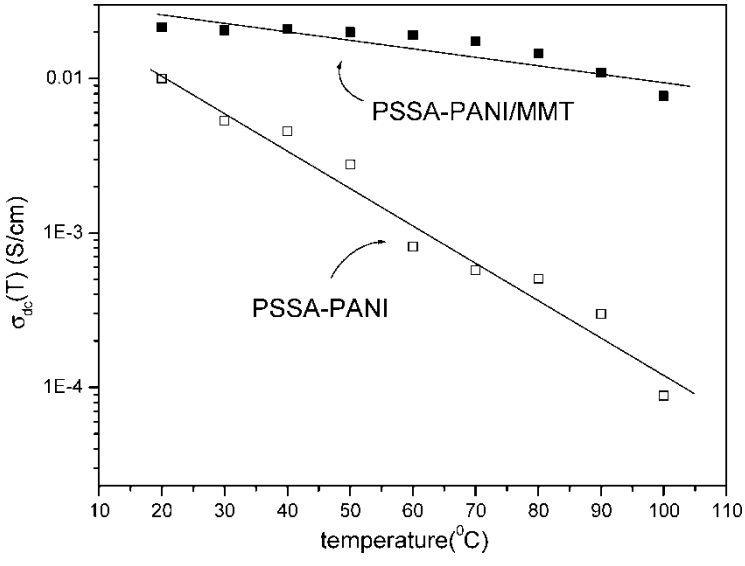

Figure 7. The temperature-dependent σ_{dc} of the PSSA-PANI and PSSA-PANI/MMT clay composite.

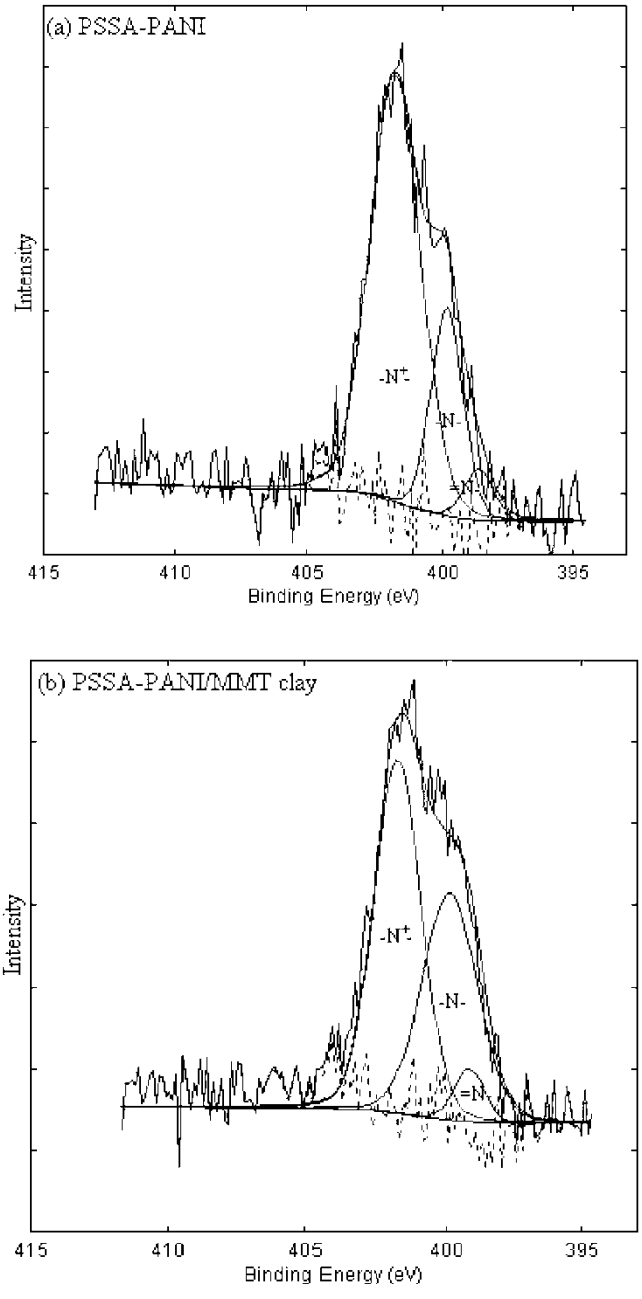

Figure 8. The N 1s XPS core level spectrum of (a) PSSA-PANI and (b) PSSA-PANI/MMT composite.

DC Conductivity

The room temperature dc conductivity [σ_{dc} (RT)] of PSSA-PANI and PSSA-PANI/MMT composite with a different PSSA molar concentration are shown in Figure 6. For PSSA-PANI samples, σ_{dc} (RT) decreases as the PSSA molar concentration increases above

0.5 M. However, σ_{dc} (RT) of PSSA-PANI/MMT decreases as the PSSA molar concentration increases above 1.25M and is higher than that of PSSA-PANI. This may be due to the interruption of the clay against the over doping which is similar with Kim et al. (28), but this effect is limited.

Figure 7 shows the temperature-dependent dc conductivity [σ_{dc}(T)] of PSSA-PANI and PSSA-PANI/MMT composite, the PSSA molar concentration of these two samples are in 1.25 M. The σ_{dc}(T) of PSSA-PANI and PSSA-PANI/MMT composite are decrease as the temperature increases, but the σ_{dc}(T) of PSSA-PANI has a sharp decrease. This result indicated again that the PSSA-PANI/MMT composite is more heat resistant than PSSA-PANI.

XPS

The N 1s XPS core level spectra of PSSA-PANI and PSSA-PANI/MMT composites are shown in Figure 8. The N 1 s main peak is decomposed into three lines. The line at 401 eV is assigned to positive nitrogen (N^+). The area ratio of N^+ component of PSSA-PANI/MMT is ~54% and lower than that of PSSA-PANI (~72%), this indicates the composites are in a low doping state (30). This also suggests the MMT clay layers interrupt the doping process.

Conclusions

We synthesized the PSSA doped water-soluble PANI/MMT clay composites. XRD patterns indicate the MMT clay in the composites has an exfoliated layered structure. The TEM photograph shows the composites has a mixed nanomorphology, some silicate layers were found to be exfoliated in the polyaniline matrix. FT-IR spectroscopy demonstrated the interaction between the PSSA-PANI chain and the surface of the MMT clay layer in the composite. This composite is more thermal stable than that without clay samples and results in good stable temperature-dependent dc conductivity [σ_{dc}(T)] as temperature changed.

References

1. Nascimento, G.M.do, Constantino, V.R.L., and Temperini, M.L.A. (2002) *Macromolecules*, 35 (20): 7535–7537.
2. Feller, J.F., Bruzaud, S., and Grohens, Y. (2004) *Materials Letters*, 58 (5): 739–745.
3. Ray, S.S. and Okamoto, M. (2003) *Prog. Polym. Sci.*, 28 (11): 1539–1641.
4. Negi, Y.S. and Adhyapak, P.V. (2002) *J. Macromol. Sci.-Polymer Reviews*, C42 (1): 35–53.
5. Wu, C.G., Liu, Y.C., and Hsu, S.S. (1999) *Synthetic Metals*, 102 (1–3): 1268–1269.
6. Gurunathan, K. and Trivedi, D.C. (2000) *Materials Letters*, 45 (5): 262–268.
7. Gurunathan, K., Amalnerkar, D.P., and Trivedi, D.C. (2003) *Materials Letters*, 57 (9–10): 1642–1648.
8. Li, X., Wang, G., Li, X., and Lu, D. (2004) *Applied Surface Science*, 229 (1–4): 395–401.
9. Khiew, P.S., Huang, N.M., Radiman, S., and Ahmad, M.S. (2004) *Materials Letters*, 58 (3–4): 516–521.
10. Kinomura, N., Toyama, T., and Kumada, N. (1995) *Solid State Ionics*, 78 (3–4): 281–286.
11. Xiao, P., Xiao, M., Liu, P., and Gong, K. (2000) *Carbon*, 38 (4): 626–628.
12. Anaissi, F.J., Demets, G.J.-F., Timm, R.A., and Toma, H.E. (2003) *Materials Science and Engineering*, A347 (1–2): 374–381.
13. Ilic, M., Koglin, E., Pohlmeier, A., Narres, H.D., and Schwuger, M.J. (2000) *Langmuir*, 16 (23): 8946–8951.

14. Orata, D. and David, S.K. (2000) *Reactive & Functional Polymers*, 43 (1–2): 133–138.
15. Orata, D. and Segor, F. (2000) *Reactive & Functional Polymers*, 43 (3): 305–314.
16. Kim, B.H., Jung, J.H., Kim, J.W., Choi, H.J., and Joo, J. (2001) *Synthetic Metals*, 121 (1–3): 1311–1312.
17. Kim, B.H., Jung, J.H., Kim, J.W., Choi, H.J., and Joo, J. (2001) *Synthetic Metals*, 117 (1–3): 115–118.
18. Yang, S.M. and Chen, K.H. (2003) *Synthetic Metals*, 135–136: 51–52.
19. Chen, K.H. and Yang, S.M. (2003) *Synthetic Metals*, 135–136: 151–152.
20. Wu, Q., Xue, Z., Qi, Z., and Wang, F. (2000) *Polymer*, 41 (6): 2029–2032.
21. Nascimento, G.M.do, Constantino, V.R.L., Landers, R., and Temperini, M.L.A. (2004) *Macromolecules*, 37 (25): 9373–9385.
22. Goddard, Y.A., Vold, R.L., and Hoatson, G.L. (2003) *Macromolecules*, 36 (4): 1162–1169.
23. Lee, D., Char, K., Lee, S.W., and Park, Y.W. (2003) *Journal of Materials Chemistry*, 13 (12): 2942–2947.
24. Lee, D. and Char, K. (2002) *Polymer Degradation and Stability*, 75 (3): 555–560.
25. Lim, Y.T., Park, J.H., and Park, O.O. (2002) *Journal of Colloid and Interface Science*, 245 (1): 198–203.
26. Yeh, J.-M., Liou, S.-J., Lai, C.-Y., and Wu, P.-C. (2001) *Chem. Mater.*, 13 (3): 1131–1136.
27. Lee, D., Lee, S.-H., Char, K., and Kim, J. (2000) *Macromol. Rapid Commun.*, 21 (16): 1136–1139.
28. Kim, B.-H., Jung, J.-H., Hong, S.-H., Joo, J., Epstein, A.J., Mizoguchi, K., Kim, J.W., and Choi, H.J. (2002) *Macromolecules*, 35 (4): 1419–1423.
29. Jia, W., Segal, E., Kornemandel, D., Lamhot, Y., Narkis, M., and Siegmann, A. (2002) *Synthetic Metals*, 128 (1): 115–120.
30. Kim, B.H., Jung, J.H., Hong, S.H., Kim, J.W., Choi, H.J., and Joo, J. (2001) *Current Applied Physics*, 1 (1): 112–115.